Electron Transfer from the S_1 and S_2 States of Pentacoordinated Tetrapyrrole Macrocycles to Pyromellitic Diimide as an Axial Ligand

Ken Harada, Mamoru Fujitsuka,* Akira Sugimoto, and Tetsuro Majima*

Institute of Scientific and Industrial Research (SANKEN), Osaka University, Mihogaoka 8-1, Ibaraki, Osaka 567-0047, Japan

Received: July 3, 2007; In Final Form: August 29, 2007

Electron transfer (ET) reactions from the S_1 and S_2 states of some porphyrins and phthalocyanines to the axial ligand have been investigated by means of femtosecond laser flash photolysis. As the axial ligand, which acts as an acceptor, we synthesized an asymmetric pyromellitic diimide (PI) compound that has an alkyl chain and a pyridine ring on N and N′ atoms, respectively. The pyridine ring of PI can coordinate to Zn of tetrapyrrole macrocycles. The coordination was confirmed by UV−vis and ^{1}H NMR spectra. ET from the S_1 state of Zn tetraphenylporphyrin (ZnTPP), Zn octaethylporphyrin (ZnOEP), Zn phthalocyanine (ZnPc), and Zn naphthalocyanine (ZnNc) to PI was confirmed with transient absorption spectroscopy by observing $PI^{\bullet-}$. ET from the S_1 state occurred at the rate constant of $(8.6\ ps)^{-1} - (78\ ps)^{-1}$, and the yield was almost unity. Furthermore, ET from the S_2 state of ZnTPP and ZnPc to PI was confirmed. ET from the S_2 state of ZnPc was observed for the first time. The ET rate from the S_2 state was faster than that from the S_1 state. In the case of ZnOEP−PI and ZnNc−PI complexes, ET from the S_2 state was not observed.

Introduction

Photosynthesis is one of the most important reactions in chemistry. In photosynthesis, light-harvesting complex captures photon and transfers its energy to the chlorophyll (Chl) special pair of the photosynthesis reaction center. The energy transfer and following electron transfer (ET) in the photosynthesis system are very efficient. Their quantum yields are almost unity. Mimicking the natural photosynthesis is an important subject to achieve the artificial photosynthesis and also to develop novel electronic devices. Because ET is the primal reaction in the reaction center, many research groups have put a lot of effort into achieving efficient and long-lived charge-separated state using donor−acceptor dyad, triad, and so on.[1] To realize the efficient ET, ET from the higher excited-state such as the S_2 state has to be also considered. Even for the donor−acceptor dyad in which ET cannot occur from the S_1 state, excitation to the S_2 state makes ET energetically possible in some cases. Tetrapyrrole macrocycles, such as tetraphenylporphyrin (TPP), octaethylporphyrin (OEP), phthalocyanine (Pc), and naphthalocyanine (Nc), are known as good model compounds of Chl because of their stability. Various research groups have reported about their energy transfer and ET from the S_1 state.[2] ET from the S_2 state of ZnTPP derivatives in which an acceptor was connected at meso- or β-position has been reported.[3] Mataga et al. reported free energy dependence of ET rate from the S_2 state.[3a] Wasielewski et al. reported 6 times faster ET from the S_2 state than ET from the S_1 state.[3b] Although the S_2 state properties of OEP, Pc, and Nc have been reported,[4] ET from their S_2 state has not been reported yet; they still have enough room to study more.

To mimic the natural photosynthesis reaction, the self-assembled supramolecular systems seem to be a good candidate as a model compound of the reaction center, because in the natural photosynthesis system, bacteriochlorophylls are arranged in a specific configuration by interactions with surrounding peptides. The BChl exists as the pentacoordinated complexes with the imidazole moiety of histizine as an axial ligand.

We report here ET from the S_1 and S_2 states of some Zn tetrapyrrole macrocycles coordinated with pyromellitic diimide. It is well known that the N atom of a pyridine ring can coordinate to the Zn atom of ZnTPP.[5] The pyromellitic diimide compound (PI) that we synthesized has the pyridine ring (Figure 1), and it can coordinate to the Zn atom of ZnTPP, ZnOEP, ZnPc, and ZnNc. PI has low reduction potential and $PI^{\bullet-}$ has an intense absorption peak at 720 nm, so PI is a useful chromophore as an electron acceptor. Figure 1 shows the structure of the ZnTPP−PI complex as a representative. Because the distance between donor and acceptor in the complex is short, ET is expected even in the S_2 state with very short lifetime.

Experimental Section

Materials. 5,10,15,20-Tetraphenyl-21*H*,23*H*-porphine zinc (ZnTPP), 2,3,7,8,12,13,17,18-octaethyl-21*H*,23*H*-porphine zinc (ZnOEP), zinc 2,9,16,23-tetra-*tert*-butyl-29*H*,31*H*-phthalocyanine (ZnPc), and zinc 2,11,20,29-tetra-*tert*-butyl-2,3-naphthalocyanine (ZnNc) were purchased from Aldrich Chemical Co. and used without further purification. Toluene (spectral grade) was purchased from Nacalai Tesque Inc.

Synthesis of *N*-(2-Ethylhexyl)-*N*′-(4-pyridyl)-pyromellitic Diimide. 2-Ethylhexylamine (1.84 g, 14.3 mmol) and 4-aminopyridine (2.68 g, 14.3 mmol) in 50 mL of dimethylformamide (DMF) were added to 150 mL of DMF including pyromellitic dianhydride (4.25 g, 19.5 mmol). The reaction mixture was stirred overnight at room temperature. After filtration, the mixture was evaporated. Acetic anhydride was added to the residue and stirred for 1 h at 100 °C. After filtration, the solvent was removed. The crude product was purified by column chromatography ($EtOAc/CH_2Cl_2$ (1/10)). The yield of PI (770

* To whom correspondence should be addressed. E-mail: (M.F.) fuji@sanken.osaka-u.ac.jp; (T.M.) majima@sanken.osaka-u.ac.jp.

10.1021/jp075153o CCC: $37.00
Published on Web 10/19/2007

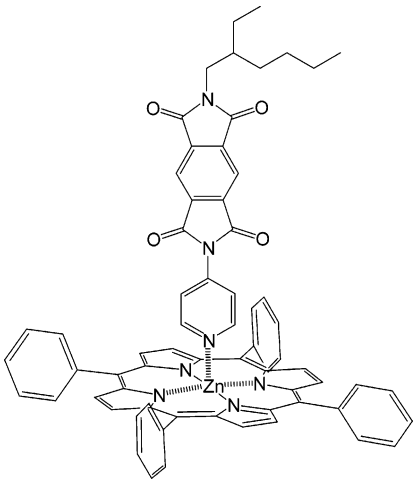

Figure 1. Structure of ZnTPP−PI complex.

mg) was 9.7%. ^{1}H NMR ($CDCl_3$): δ 8.80 (d, J = 4.86 Hz, 2H); 8.41(s, 2H); 7.62 (d, J = 4.86 Hz, 2H); 3.67 (d, J = 7.29 Hz, 2H); 1.87 (m, 1H); 1.25 (m, 8H); 0.90 ppm (m, 6H). FAB-MS: 407 (405.2, calcd).

General Method. In the transient absorption measurements, complexes were prepared using excess amount of PI. Judging from the association constant (vide infra), almost all tetrapyrrole macrocycles were in the complex form.

Apparatus. The steady state absorption and fluorescence spectra were measured using Shimadzu UV-3100PC and Hitachi 850, respectively. ^{1}H NMR spectra were measured in $CDCl_3$ or $C_6D_5CD_3$ at room temperature using a JEOL JMN LA-400.

The subpicosecond transient absorption spectra were measured by the pump and probe method using a regeneratively amplified titanium sapphire laser (Spectra Physics, Spitfire Pro F, 1 kHz) pumped by a Nd:YLF laser (Spectra Physics, Empower 15). The seed pulse was generated by the titanium sapphire laser (Spectra Physics, Tsunami 3941-M1BB, full width at half-maximum (fwhm) 80 fs, 800 nm). The second harmonic oscillation (400 nm, 130 fs fwhm, 8 μJ pulse^{-1}) of the output of the regeneratively amplified titanium sapphire laser was used as the excitation pulse. Excitation pulse at 540, 570, and 680 nm was generated by optical parametric amplifier (Spectra Physics, OPA-800CF). A white continuum pulse, which was generated by focusing the residual of the fundamental light to a flowing water cell after a computer-controlled optical delay, was divided into two parts and used as the probe and the reference lights, of which the latter was used to compensate the laser fluctuation. The both probe and reference lights were directed to a rotating sample cell with 1.0 mm of optical path and were detected with a charge-coupled device detector equipped with a polychromator (Solar, MS3504). The pump pulse was chopped by a mechanical chopper synchronized to one-half of the laser repetition rate, resulting in a pair of the spectra with and without the pump, from which absorption change induced by the pump pulse was estimated.

Optimized structures of ZnTPP−PI, ZnOEP−PI, ZnPc−PI, and ZnNc−PI were estimated at the B3LYP/6-31G* level using the Gaussian 03 package.[6]

Results and Discussion

Absorption and Fluorescence Spectra. When PI in toluene was added dropwise to toluene solution of ZnTPP, steady state absorption showed obvious changes;[5] Soret and Q-bands were red-shifted by 6 and 11 nm, respectively, with isosbestic points

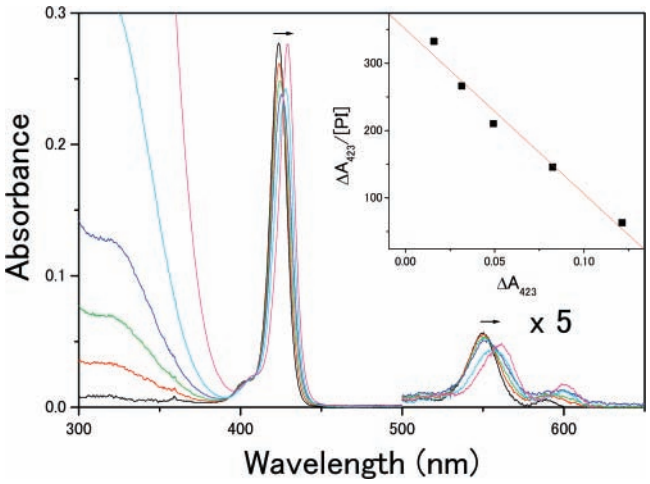

Figure 2. UV−vis absorption spectra observed during the complexation of PI and ZnTPP in toluene at room temperature. 4, 15, 20, 50, and 200 μL of PI solution (9.6 mM) was added to ZnTPP solution (3.1 μM). The inset shows the Scatchard plot of absorbance at 423 nm.

at 426 and 555 nm (Figure 2). These spectral changes are clear evidence for the generation of pentacoordinated ZnTPP,[5] that is, PI is coordinated to central Zn as illustrated in Figure 1, because these spectral changes were also observed for the complex of pyridine (Py) and ZnTPP. Similar spectral changes were confirmed for ZnOEP and ZnPc. In the case of ZnNc complex, Q-bands were blue-shifted (see Supporting Information).

From the absorption spectral data, the association constant, K_a, was estimated by using the Scatchard method.[7] The estimated K_a values are listed in Table 1. From these values, PI can coordinate to the Zn atom of tetrapyrrole macrocycles easier than Py except for ZnPc.[8−10] As indicated in the Experimental Section, PI was added to tetrapyrrole macrocycles by a factor of 10^3 for the transient absorption measurements. Under this condition, >96% of tetrapyrrole macrocycles are in the pentacoordinated form.

For all macrocycles, when PI was added to tetrapyrrole macrocycles, intensities of fluorescence from the S_1 state decreased compared to the complexes with Py. Decrease of fluorescence intensity was also confirmed for S_2 fluorescence of ZnTPP. This implies that ET from macrocycles to PI occurred.

^{1}H NMR Spectra. Another evidence for the complexation was obtained from ^{1}H NMR spectra as shown in Figure 3. The spectra revealed that the peaks due to H of PI were shifted when PI formed a complex. The δ values of the H of PI were 8.80 (H_a), 8.41 (H_c), and 7.62 (H_b) ppm in $CDCl_3$. When ZnTPP and PI formed the complex, the peaks were shifted to lower field. In the case of ZnTPP−PI, when 0.46 equiv of PI was added to ZnTPP in $CDCl_3$, H_b was observed at δ = 6.34 ppm (Figure 3B). When 6.7 equiv of PI was added, the H_b was shifted to δ = 7.52 ppm (Figure 3G). Other protons also showed the peak shift, especially H_a, H_b, and H_c, which showed a relatively large shift, indicating the complexation at the pyridine ring of PI to ZnTPP. ZnOEP in $CDCl_3$ and ZnPc in $C_6D_5CD_3$ showed similar results, but ZnNc did not show clear spectra because of its low solubility (see Supporting Information).

Molecular Orbital Calculation. Structures of the complexes were estimated by molecular orbital calculation. The optimized structure of ZnTPP−PI is shown in Figure 4. The optimized structures of the other complexes were shown in Supporting Information. Figure 4 indicates that highest occupied molecular

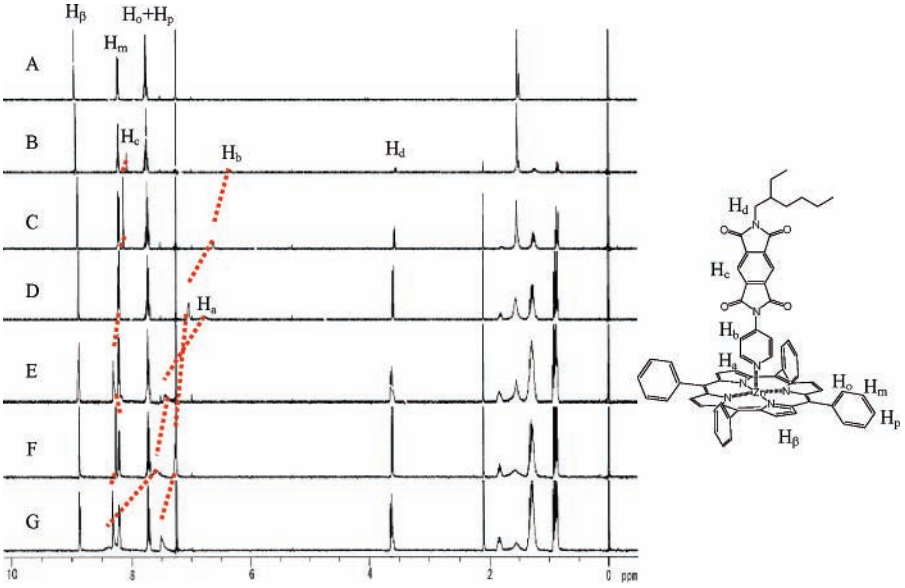

Figure 3. ^{1}H NMR spectra of ZnTPP−PI. (A) ^{1}H NMR spectra of ZnTPP in $CDCl_3$. (B−G) 0.46, 0.86, 2.2, 4.1, 4.6, and 6.7 equiv of PI.

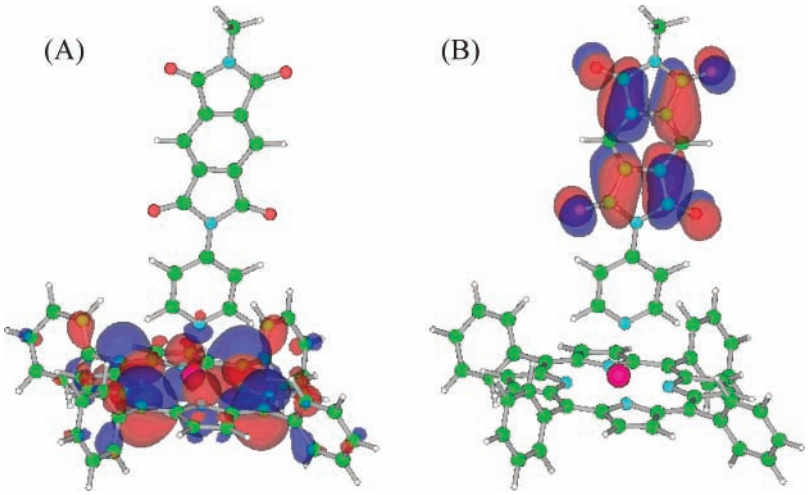

Figure 4. Structure of the complex of ZnTPP and PI. Optimized structures of the complex were estimated at the B3LYP/6-31G* level with the Gaussian 03 package. HOMO was shown in (A) and LUMO in (B). Alkyl group of PI was reduced to methyl group.

TABLE 1: The Absorption Peaks and the Association Constants, K_a, in Toluene Obtained from the Scatchard Method at Room Temperature

	λ_{max}/nm			K_a / M^{-1}	
	without complexation	complex with Py	complex with PI	Py	PI
ZnTPP	423, 550, 587	429, 562, 601	429, 561, 600	1000	2400
ZnOEP	405, 533, 570	415, 542, 577	414, 542, 576	2200	2500
ZnPc	349, 611, 677	352, 611, 678	−[a], 611, 678	51000	8400
ZnNc	340, 686, 731, 769	340, 684, 730, 767	−[a], 685, 730, 769	9100	86000

[a] The data was not obtained because the absorption of macrocycles was overlapped with the absorption of PI.

orbital (HOMO) is localized on ZnTPP, donor, and lowest unoccupied molecular orbital (LUMO) on PI, acceptor. Thus, when the complex is excited, ET from ZnTPP to PI might occur. LUMO is localized on the pyromellitic diimide and not on the pyridine ring. Thus the pyridine ring acts as a spacer in the ET process.

From the optimized structure of ZnTPP−PI, the center-to-center distance of donor and acceptor was 10.2 Å. For other complexes the center-to-center distance was 10.2−10.3 Å. This implies that the distance is almost the same. The electron density of donor and acceptor has important effects on the ET rate.[3b,11] From the optimized structure, LUMO was also localized on the carbonyl groups of PI. The distance between the O atom and macrocycle plane was 7.22−7.30 Å, independent of macrocycles. With the formation of the pentacoordinated Zn ion, Zn ion is slightly pulled out from the tetrapyrrole macrocycle plane by 0.38−0.53 Å. These structural parameters are summarized in Table S1 of Supporting Information.

Electrochemistry. To estimate the driving force ($-\Delta G$) for the ET from the S_1 and S_2 states, the oxidation potentials of the complexes with Py as model compounds were measured by the cyclic voltammetry. The redox potentials are summarized in

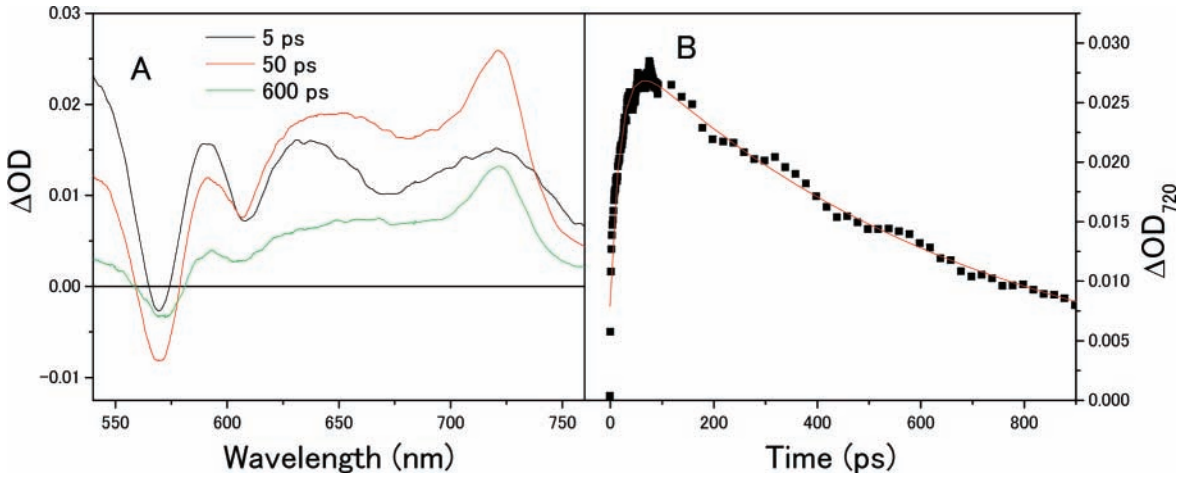

Figure 5. (A) Transient absorption spectra of ZnTPP−PI complex in toluene excited at 570 nm. (B) Time profile at 720 nm. The red line is the fitted curve.

TABLE 2: The Data of Redox Potential and Driving Force, $-\Delta G$, for ET in the Complex with PI

	E_{ox}[a]/V vs SCE	E_{red}[a]/V vs SCE	$E_{00}(S_1)$eV	$E_{00}(S_2)$/eV	$-\Delta G(S_1)$/eV	$-\Delta G(S_2)$/eV	$-\Delta G$(CR)/eV
PI		−0.83					
ZnTPP−Py	0.57		1.88	2.81	0.83	1.76	1.05
ZnOEP−Py	0.61		2.13	2.83[b]	1.04	1.74	1.09
ZnPc−Py	0.57		1.79	2.72[b]	0.74	1.67	1.05
ZnNc−Py	1.15		1.82	2.30[b]	0.19	0.67	1.63

[a] The redox potentials were obtained using cyclic voltammetry in 50 mM $TEAClO_4$ dichloromethane. Scan rate was 100 mV s^{-1}. [b]These values were estimated from the absorption tail of the Soret band.

Table 2. The $-\Delta G$ values were estimated from eqs 1 and 2[12]

$$-\Delta G = E_{red} - E_{ox} + E_{00} + \Delta G_S \quad (1)$$

$$\Delta G_S = e^2\left(\frac{1}{2r_D} + \frac{1}{2r_A}\right)\left(\frac{1}{\epsilon_s} - \frac{1}{\epsilon_r}\right) - \frac{e^2}{\epsilon_s r} \quad (2)$$

where r_D and r_A are the effective radii of the donor$^{\bullet+}$ and acceptor$^{\bullet-}$ ions and are reported to be 5 (ZnTPP) and 3.5 Å (pyromellitic diimide), respectively.[12] ϵ_r is the dielectric constant of CH_2Cl_2 and the ϵ_s is that of toluene. The r is the center-to-center distance. The energy level, E_{00}, was estimated from the peak of fluorescence spectra except for $E_{00}(S_2)$ of ZnOEP−Py, ZnPc−Py, and ZnNc−Py. Because of the absence of S_2-fluorescence, their $E_{00}(S_2)$ values were obtained from the absorption tail of the Soret band. Thus, these values might have some error. It is reported that eq 2 gives too large ΔG_s in nonpolar solvent, such as toluene. The calculated value of ΔG_s was decreased to 0.35 eV as indicated in ref 12. These $-\Delta G$ values indicate that ET is possible both from the S_1 and S_2 states.

Charge Separation (CS) from the S_1 State. The photoinduced process of ZnTPP−PI in toluene was investigated by excitation of the sample with a 570 nm laser pulse that excites the Q-band of ZnTPP generating the S_1 state of ZnTPP. The obtained transient absorption spectra and time profile of PI$^{\bullet-}$ at 720 nm[3b] of the ZnTPP−PI complex are shown in Figure 5. At 5 ps after excitation, a spectrum of S_1-excited ZnTPP was observed. After that, PI$^{\bullet-}$ (720 nm) showed maximal concentration around 70 ps and disappeared with $(690\ ps)^{-1}$ of the time constant.

Photoinduced process of ZnPc−PI upon excitation to the S_1 state in toluene was investigated by excitation of the sample with 680 nm laser pulse. The CS was confirmed by appearance of PI$^{\bullet-}$ (720 nm) and ZnPc$^{\bullet+}$ (850 nm) (Figure 6).[14] The peak of PI$^{\bullet-}$ appeared at $(82\ ps)^{-1}$, and its lifetime was in nanosecond order.

For ZnOEP−PI and ZnNc−PI, CS from the S_1 state was also confirmed (Figure S10 and S11 of Supporting Information). The CS rate constants were estimated by subtraction of radiative and internal conversion rates from the apparent rate. CS and charge recombination (CR) rates are summarized in Table 3. The lifetime of the S_1 state of ZnTPP, ZnOEP, ZnPc, and ZnNc was reported to be 2.4, 2.0, 3.6, and 2.4 ns, respectively.[3b,15−17] From these values, it is revealed that the ET from the S_1 state occurred very efficiently in all cases. The quantum yields of ET from the S_1 state (Φ_{CS1}) were almost unity in all cases (Table 3). Because time profile of ZnPc transient absorption at 720 nm did not show substantial decay within our instrumental measurable range at 720 nm, k_{CR} of ZnPc may have some error.

In Figure 7, observed CS and CR rates, k_{ET}, were plotted against the driving force. Roughly saying, Figure 7 suggests that ET from the S_1 state occurred on a similar Marcus parabola except for CR in ZnNc−PI complex. Although CR processes have a larger driving force, CR rates were slower than CS rates. This implies that CR processes were in the Marcus inverted region. The reorganization energy will be 0.1−0.8 eV. In Figure 7, a tentative Marcus parabola is drawn by assuming 0.5 eV and 30 cm^{-1} of reorganization energy and coupling matrix element, respectively. The results show that the ET from the S_1 state occurred in Marcus top and normal region resulting in very efficient ET. Opened symbols are the ET rate from the S_2 state (vide infra).

CS from the S_2 State. When the ZnTPP−PI was excited to the S_2 state by 400 nm laser pulse, the peak of PI$^{\bullet-}$ appeared obviously faster than the S_1-excitation (Figure 8 and Supporting Information.). This implies that the ET occurred from the S_2 state in this complex. The apparent rate of ET from the S_2 state was estimated to be $(4.8\ ps)^{-1}$. The CS rate constant was estimated by the similar manner to that from the S_1 state (Table 4). It was 5.5 times faster than ET from the S_1 state. Because the S_2-fluorescence lifetime of ZnTPP is reported to be 2.4−3

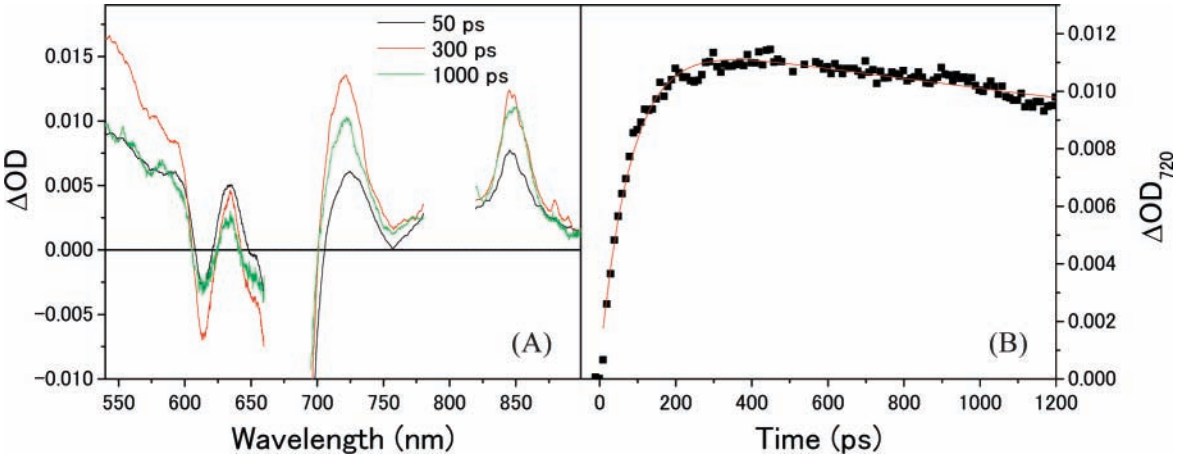

Figure 6. (A) Transient absorption spectra of ZnPc−PI complex in toluene excited at 680 nm. (B) Time profile at 720 nm excited at 680 nm. The red line is the fitted curve.

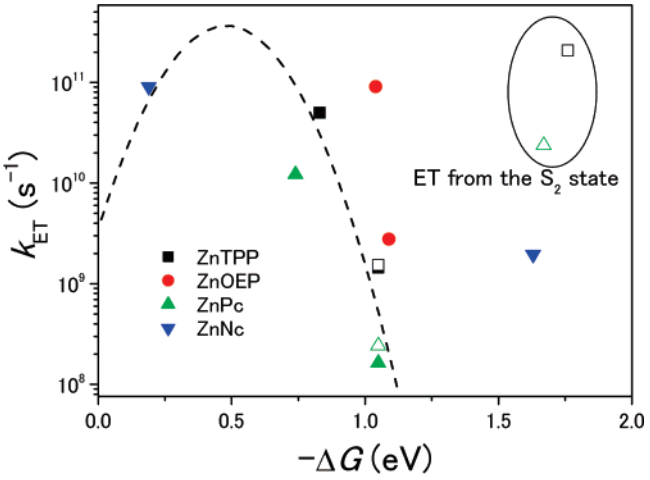

Figure 7. The plots of rate constants, k_{ET}, against $-\Delta G$. Opened symbols are ET rate from the S_2 state. The broken line is a tentative Marcus parabola by assuming 0.5 eV and 30 cm^{-1} of reorganization energy and coupling matrix element, respectively.

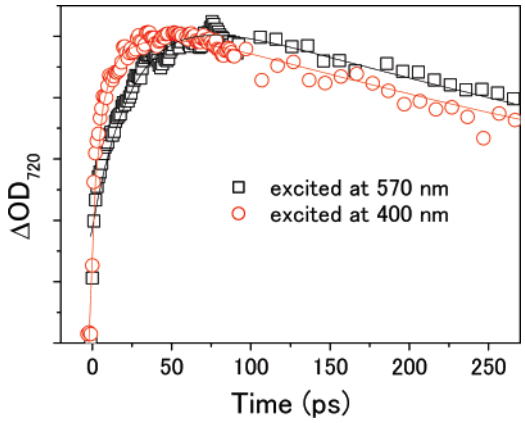

Figure 8. Time profiles of ZnTPP−PI complex in short time scale. Excitation wavelength: 400 nm (circle) and 570 nm (square). The black and red lines were fitted curves.

ps,[15] the CS is not an efficient process due to the other deactivation processes such as internal conversion. Thus the quantum yield of ET from the S_2 state is as low as 0.63 (Table 4).

The ET from the S_2 state was also confirmed for ZnPc−PI. When the complex was excited to the S_2 state by 400 nm laser pulse, the peak of $PI^{\bullet-}$ appeared with two components of (42 ps)$^{-1}$ and (82 ps)$^{-1}$ (Figure 9 and Supporting Information). When the complex was excited at 680 nm, the peak of $PI^{\bullet-}$ appeared at (82 ps)$^{-1}$. So ET from the S_2 state of ZnPc occurred at (42 ps)$^{-1}$. It was 2.0 times faster than ET from the S_1 state. Because the lifetime of the S_2 state of ZnPc−Py was estimated to be 14 ps (Supporting Information), the quantum yield of ET from the S_2 state was estimated to be 0.33. Thus, CS from the S_2 state is also a minor process in S_2 excited ZnPc−PI.

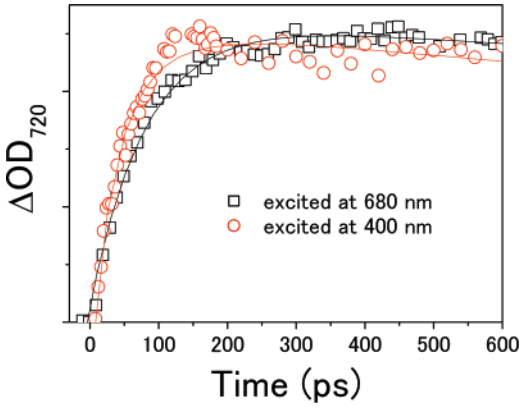

Figure 9. Time profiles of ZnPc−PI complex in short time scale. Excitation wavelength: 400 nm (circle) and 680 nm (square). The black and red lines were fitted curves.

TABLE 3: Summary of Transient Absorption and Kinetic Data of ET from the S_1 State[a]

compound	λ_{EX}/nm	λ_{PR}/nm	τ_{CS1}/ps	τ_{CR}/ps	Φ_{CS1}/%
ZnTPP−PI	570	720	18	690	99
ZnOEP−PI	540	720	9.0	360	100
ZnPc−PI	680	720	78	6100	98
ZnNc−PI	680	980	8.6	510	100

[a] λ_{EX} and λ_{PR} are excitation and probe wavelengths, respectively. τ_{CS1} and τ_{CR} are the rate constants of CS from the S_1 state and CR, respectively.

TABLE 4: Summary of Transient Absorption and Kinetic Data of ET from the S_2 State[a]

compound	λ_{EX}/nm	λ_{PR}/nm	τ_{CS2}/ps	τ_{CS1}/ps	τ_{CR}/ps	Φ_{CS2}/%
ZnTPP−PI	400	720	1.8	22	650	63[b]
ZnPc−PI	400	720	28	78	4100	33

[a] λ_{EX} and λ_{PR} are excitation and probe wavelengths, respectively. τ_{CS1} and τ_{CS2} are the time constants of the CS from the S_1 state and the S_2 state, respectively, while τ_{CR} is the time constant of CR. [b]Calculated with the assumption that the lifetime of ZnTPP S_2 state was 3 ps.[15]

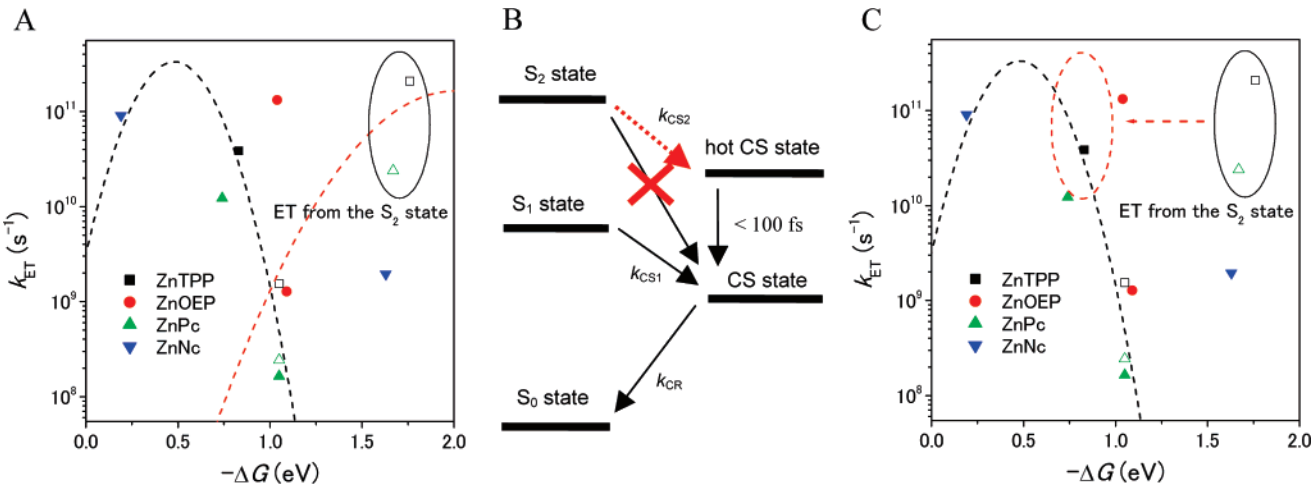

Figure 10. (A) The rate constants, k_{ET}, were plotted against $-\Delta G$ under the assumption that ET from the S_2 state was on another Marcus parabola from ET from the S_1 state. The red curve was drawn with larger reorganization energy ($\lambda = 2.0$ eV). (B) The energy level diagram of the complex including the hot CS state. (C) The rate constants, k_{ET}, were plotted against $-\Delta G$ under the assumption that ET from the S_2 state has smaller -ΔG.

In the cases of ZnOEP−PI and ZnNc−PI, $PI^{\bullet-}$ appeared in almost the same time scale as the S_1-excitation. From the results, ET from the S_2 state was not obvious, probably because internal conversion from the S_2 state to the S_1 state occurred rapidly. In the case of ZnOEP, the S_2-state lifetime was reported to be $<10^{-2}$ ps.[16] The lifetime of the S_2 state of ZnNc−Py was estimated to be 1.6 ps (Figure S15 of Supporting Information). In addition, that ZnNc complex has lower $-\Delta G$ for CS compared to the other complexes. Thus, CS from the S_2 state was difficult to observe.

Mataga et al. observed ET from the S_2 state of Zn porphyrin to pyromellitic diimide directly linked at meso position. The rate constant of ET from the S_2 state was larger than $(0.5\ ps)^{-1}$, because the dyad has a very short center-to-center distance, such as 3.5 Å.[3a] Wasielewski et al. reported ET from the S_2 state of ZnTPP to covalently bound PI. The rate constants for the dyad linked by a phenyl ring at the meso position and β-position of ZnTPP dyads were $(1.3\ ps)^{-1}$ and $(0.63\ ps)^{-1}$, respectively. The quantum yields were 0.46 and 0.64, respectively. The difference between the rate constants of CS caused from the difference of the electron density at meso and β-positions.[3b] Thus, one of the reasons for the slow ET in our supramolecular dyads should be longer distance between donor and acceptor. The absence of HOMO density on the Zn atom also decreases the ET rate.

In Figure 9, the ET rate from the S_2 state was also plotted against driving force. It is clear that the ET rate from the S_2 state was not on the Marcus parabola for ET from the S_1 state. This is a quite unique feature for ET from the S_2 state. As a reason for this behavior, the following two possibilities can be pointed out. First, ET from the S_2 state was not on the Marcus parabola for ET from the S_1 state. To explain the ET rate from the S_2 state, Marcus parabola with larger reorganization energy should be considered. Because solvent reorganization energy may not depend on excited state, internal reorganization energy varies to much extent. That is, when the complexes were excited to the S_2 state, their structures might change larger than S_1-excitation. By assuming $\lambda = 2.0$ eV, Marcus parabola can be drawn as the red line in Figure 10A. Second, ET from the S_2 state to the hot CS state will be another possible ET process (Figure 10B). In this case, $-\Delta G_{CS}$ value should be smaller as indicated in Figure 10C.[19] Thus, $-\Delta G(S_2)$ in Table 2 may be overestimated. But the CR rates do not have a difference between S_1-excitation and S_2-excitation. Thus, relaxation rate from the hot CS state to the CS state should be quite fast. The rate will be <100 fs because the transient absorption spectra attributable to the hot CS was not observed.[19] When the plots of ET from the S_2 state were shifted to the Marcus parabola of ET from the S_1 state, $-\Delta G(S_2)$ was decreased to 0.6−0.9 eV and the energy difference between the hot CS state and the CS state can be estimated 0.8−1 eV. From the absence of corresponding electronic transition both in $ZnTPP^{\bullet+}$ and $PI^{\bullet-}$, the higher vibration state of the complexes should be included in the CR process. To distinguish these possibilities, detailed study on free energy dependence of the electron-transfer rates is needed. Such a study will be done in the next stage of our work.

Conclusions

For the supramolecular dyad of tetrapyrrole macrocycles, CS from the S_1 state was confirmed. The CS occurred in the Marcus normal and top regions, and the CR in the Marcus inverted region. We also revealed the ET from the S_2 state of ZnTPP and ZnPc to PI. Although the ET from the S_1 state occurred very efficiently, the ET from the S_2 state was not so efficient because of their short lifetime of the S_2 states. ET from the S_2 state of ZnPc was observed for the first time. These results also suggest that two types of ET can occur in these complexes, and it depends on excitation wavelength.

Acknowledgment. This work has been partly supported by a Grant-in-Aid for Scientific Research (Project 17105005, 19350069, and others) from the Ministry of Education, Culture, Sports, Science, and Technology (MEXT) of the Japanese Government.

Supporting Information Available: UV-vis spectral changes observed during the complexation with PI in toluene, ^{1}H-NMR spectra, molecular orbital calculation, transient absorption spectra, and evaluation of S_2 state lifetimes. This material is available free of charge via the Internet at http://pubs.acs.org.

References and Notes

(1) (a) Miller, S. E.; Lukas, A. S.; Marsh, E.; Bushard, P.; Wasielewski, M. R. *J. Am. Chem. Soc.* **2000**, *122*, 7802−7810. (b) Wasielewski, M. R. *Chem. Rev.* **1992**, *92*, 435−461. (c) Steinberg-Yfrach, G.; Liddell, P. A.; Hung, S.-C.; Moore, A. L.; Gust, D.; Moore, T. A. *Nature* **1997**, *385*, 239−241. (d) Campidelli, S.; Sooambar, C.; Lozano-Diz, E.; Ehli, C.; Guldi, D. M.; Prato, M. *J. Am. Chem. Soc.* **2006**, *128*, 12544−12552. (e) Beckers, E. H. A.; Meskers, S. C. J.; Schenning, A. P. H. J.; Chen, Z.; Wurthner, F.;

Janssen, R. A. J. *J. Phys. Chem. A* **2004**, *108*, 6933−6937. (f) Lewis, F. D.; Wu, Y.; Zhang, L.; Zuo, X.; Hayes, R. T.; Wasielewski, M. R. *J. Am. Chem. Soc.* **2004**, *126*, 8206−8215. (g) Choi, M.-S.; Aida, T.; Luo, H.; Araki, Y.; Ito, O. *Angew. Chem., Int. Ed.* **2003**, *42*, 4060−4063.

(2) (a) Huang, Q.; Sandanayaka, A. S. D.; Bando, Y.; Zhi, C.; Ma, R.; Shen, G.; Golberg, D.; Zhao, J.; Araki, Y.; Ito, O.; Gao, L. *Adv. Mater.* **2007**, *19*, 934−938. (b) Ito, F.; Ishibashi, Y.; Khan, S. R.; Miyasaka, H.; Kameyama, K.; Morisue, M.; Satake, A.; Ogawa, K.; Kobuke, Y. *J. Phys. Chem. A* **2006**, *110*, 12734−12742. (c) Ahrens, M. J.; Kelley, R. F.; Dance, Z. E. X.; Wasielewski, M. R. *Phys. Chem. Chem. Phys.* **2007**, *9*, 1469−1478. (d) Ballesteros, B.; de la Torre, G.; Ehli, C.; Aminur Rahman, G. M.; Agullo-Rueda, F.; Guldi, D. M.; Torres, T. *J. Am. Chem. Soc.* **2007**, *129*, 5061−5068. (e) Chitta, R.; Sandanayaka, A. S. D.; Schumacher, A. L.; D'Souza, L.; Araki, Y.; Ito, O.; D'Souza, F. *J. Phys. Chem. C* **2007**, *111*, 6947−6955. (f) Berera, R.; Herrero, C.; Stokkum, I. H. M. V.; Vengris, M.; Kodis, G.; Palacios, R. E.; Amerongen, H. V.; Grondelle, R. V.; Gust, D.; Moore, T. A.; Moore, A. L.; Kennis, J. T. M. *Proc. Natl. Acad. Sci. U.S.A.* **2006**, *103*, 5343−5348. (g) Galloni, P.; Floris, B.; De Cola, L.; Cecchetto, E.; Williams, R. M. *J. Phys. Chem. C* **2007**, *111*, 1517−1523. (h) Hasselman, G. M.; Watson, D. F.; Stromberg, J. R.; Bocian, D. F.; Holten, D.; Lindsey, J. S.; Meyer, G. J. *J. Phys. Chem. B* **2006**, *110*, 25430−25440. (i) Hodgkiss, J. M.; Damrauer, N. H.; Presse, S.; Rosenthal, J.; Nocera, D. G. *J. Phys. Chem. B* **2006**, *110*, 18853−18858.

(3) (a) Mataga, N.; Tniguchi, S.; Chosrowjan, H.; Osuka, A.; Kurotobi, K. *Chem. Phys. Lett.* **2005**, *403*, 163−168. (b) Hayes, R. T.; Walsh, C. J.; Wasielewski, M. R. *J. Phys. Chem. A* **2004**, *108*, 2375−2381.

(4) (a) Tokumaru, K. *J. Porphyrins Phthalocyanines* **2001**, *5*, 77−86. (b) Morisue, M.; Haruta, N.; Kalita, D.; Kobuke, Y. *Chem.—Eur. J.* **2006**, *12*, 8123−8135.

(5) D' Souza, F.; Ito, O. *Coord. Chem. Rev.* **2005**, *249*, 1410−1422.

(6) Frisch, M. J.; Trucks, G. W.; Schlegel, H. B.; Scuseria, G. E.; Robb, M. A.; Cheeseman, J. R.; Montgomery, J. A., Jr.; Vreven, T.; Kudin, K. N.; Burant, J. C.; Millam, J. M.; Iyengar, S. S.; Tomasi, J.; Barone, V.; Mennucci, B.; Cossi, M.; Scalmani, G.; Rega, N.; Petersson, G. A.; Nakatsuji, H.; Hada, M.; Ehara, M.; Toyota, K.; Fukuda, R.; Hasegawa, J.; Ishida, M.; Nakajima, T.; Honda, Y.; Kitao, O.; Nakai, H.; Klene, M.; Li, X.; Knox, J. E.; Hratchian, H. P.; Cross, J. B.; Bakken, V.; Adamo, C.; Jaramillo, J.; Gomperts, R.; Stratmann, R. E.; Yazyev, O.; Austin, A. J.; Cammi, R.; Pomelli, C.; Ochterski, J. W.; Ayala, P. Y.; Morokuma, K.; Voth, G. A.; Salvador, P.; Dannenberg, J. J.; Zakrzewski, V. G.; Dapprich, S.; Daniels, A. D.; Strain, M. C.; Farkas, O.; Malick, D. K.; Rabuck, A. D.; Raghavachari, K.; Foresman, J. B.; Ortiz, J. V.; Cui, Q.; Baboul, A. G.; Clifford, S.; Cioslowski, J.; Stefanov, B. B.; Liu, G.; Liashenko, A.; Piskorz, P.; Komaromi, I.; Martin, R. L.; Fox, D. J.; Keith, T.; Al-Laham, M. A.; Peng, C. Y.; Nanayakkara, A.; Challacombe, M.; Gill, P. M. W.; Johnson, B.; Chen, W.; Wong, M. W.; Gonzalez, C.; and Pople, J. A. *Gaussian 03*, Revision C.02; Gaussian, Inc.: Wallingford, CT, 2004.

(7) Scatchard, G. *Ann. N. Y. Acad. Sci.* **1949**, *51*, 660−672.

(8) Prodi, A.; Chiorboli, C.; Scandola, F.; Iengo, E.; Alessio, E.; Dobrawa, R.; Wurthner, F. *J. Am. Chem. Soc.* **2005**, *127*, 1454−1462.

(9) Ishii, K.; Ishizaki, T.; Kobayashi, N. *J. Chem. Soc., Dalton Trans.* **2001**, 3227−3231.

(10) Guldi, D. M.; Zilbermann, I.; Gouloumis, A.; Vázquez, P.; Tprres, T. *J. Phys. Chem. B* **2004**, *108*, 18485−18494.

(11) Kelley, R. F.; Shin, W. S.; Rybtchinski, B.; Sinks, L. E.; Wasielewski, M. R. *J. Am. Chem. Soc.* **2007**, *129*, 3173−3181.

(12) Mataga, N.; Chosrowjan, H.; Taniguchi, S.; Shibata, Y.; Yoshida, N.; Osuka, A.; Kikuzawa, T.; Okada, T. *J. Phys. Chem. A* **2002**, *106*, 12191−12201.

(13) Wiberg, J.; Guo, L.; Pettersson, K.; Nilsson, D.; Ljungdahl, T.; Martensson, J.; Albinsson, B. *J. Am. Chem. Soc.* **2007**, *129*, 155−163.

(14) Gouloumis, A.; de la Escosura, A.; Vazquez, P.; Torres, T.; Kahnt, A.; Guldi, D. M.; Neugebauer, H.; Winder, C.; Drees, M.; Sariciftci, N. S. *Org. Lett.* **2006**, *8*, 5187−5190.

(15) El-Khouly, M. E.; Rogers, L. M.; Zandler, M. E.; Suresh, G.; Fujitsuka, M.; Ito, O.; D'Souza, F. *Chem. Phys. Chem.* **2003**, *4*, 474−481.

(16) Liu, X.; Yeow, E. K. L.; Velate, S.; Steer, R. P. *Phys. Chem. Chem. Phys.* **2006**, *8*, 1298−1309.

(17) Guldi, D. M.; Zilbermann, I.; Gouloumis, A.; Vazquez, P.; Torres, T. *J. Phys. Chem. B* **2004**, *108*, 18485−18494.

(18) Howe, L.; Zhang, J. Z. *J. Phys. Chem. A* **1997**, *101*, 3207−3213.

(19) Beckers, E. H. A.; Meskers, S. C. J.; Schenning, A. P. H. J.; Chen, Z.; Wurthner, F.; Janssen, R. A. J. *J. Phys. Chem. A* **2004**, *108*, 6933−6937.